31st Annual International Conference of the IEEE EMBS
Minneapolis, Minnesota, USA, September 2-6, 2009

Characteristics of motion artifacts in cardiac optical mapping studies

Martin Svrcek, Sally Rutherford, Andy Y.H. Chen, Ivo Provaznik, *Member, IEEE* and Bruce Smaill

***Abstract*—Motion artifacts are one of the issues in cardiac optical mapping studies. This paper is focused on the description of the motion artifacts caused by planar movement. The theory of its origin and possibilities of its suppression is described. The suppression of the motion artifacts is based on image registration techniques. There are introduced the characteristics about influence of the weighted area averages on presence of these artifacts. In this study conventional pharmacological or mechanical ways of motion artifacts suppression were not involved.**

I. Introduction

Optical mapping is widely used in experimental studies of cardiac electrophysiology. The approach utilizes cell membrane-bound dyes, which emit fluorescence that is modulated by small changes in transmembrane potential.

Optical mapping has a number of advantages over conventional extracellular recording. Optical signals are acquired without physical contact, are directly affected by local transmembrane potential and may be recorded at high spatial density and in the presence of defibrillation-strength shocks[1]. However, optical signal quality is degraded by motion artifacts, photo-bleaching and high frequency noise.

In practice, it is necessary to minimize motion artifacts in order to record reliable action potentials using cardiac optical mapping. Typically, this is achieved by restraining heart wall motion physically or, more commonly, by employing the pharmacological agents 2,3-BDM or Cytochalasin D to block excitation-contraction coupling. Although widely used for this purpose, these uncoupling agents directly affect cardiac electrophysiology at the concentrations necessary to block contraction. An alternate approach has been to utilize the fact that, in ratiometric dyes such as di-4-ANEPPS, voltage-dependent modulation occurs in opposite directions on either side of the isobestic frequency, whereas changes due to motion and photo-bleaching do not. By recording such fluorescence signals across two wavelength windows, it is possible to minimize motion and photo-bleaching artifacts in the absence of pharmacological uncouplers using ratiometry [2] or subtraction techniques [3]. However, while these methods remove motion signal they do not correct for the loss of spatial registration that occurs during contraction.

In this study, we seek to investigate image-based transformations that can be used to preserve the spatial registration of optical mapping data recorded in the presence of cardiac wall motion.

Manuscript received April 4, 2009. This work was supported by the grants 102/07/P521 and 102/07/1473 from GACR, and by Research programme of Brno University of Technology MSM 0021630513.

M. Svrcek, is with the Brno University of Technology, Department of Biomedical Engineering, 61200 Brno, CR (phone: 0064-2102356065; e-mail: martin.svrcek@phd.feec.vutbr.cz).

S. Rutherford is with the University of Auckland, Auckland Bioengineering Institute, 1142 Auckland, NZ (e-mail: s.rutherford@auckland.ac.nz).

A. Y .T. Chen is with the University of Auckland, the Department of Physics, 1142 Auckland, NZ (e-mail: g8andy@gmail.com).

B. H. Smaill is with the University of Auckland, Auckland Bioengineering Institute, 1142 Auckland, NZ (e-mail: b.smaill@auckland.ac.nz).

I. Provaznik is with the Brno University of Technology, Department of Biomedical Engineering, 61200 Brno, CR(e-mail: provazni@feec.vutbr.cz).

II. METHODS

A. Isolated heart preparation

Rats were anesthetized and their hearts were rapidly excised and immersed in cold (4°C) saline. The aorta was cannulated, and the heart mounted on a Langendorff system and perfused with modified Krebs-Hensleit solution containing (in mM NaCl 118, KCl 4.75, $MgSO_4$ 1.18, KH_2PO_4 1.18, $NaHCO_3$ 24.8, Glucose 10, $CaCl_2$ 2.5) and perfused at room temperature at a constant pressure ~80mmHg. The hearts were stabilized for 30 minutes. The coronary circulation was loaded with voltage sensitive dye di-4-ANEPPS (Molecular Probes) at ~100 μM for 5 minutes.

B. Optical system

The heart was illuminated with 2 blue LEDs (Luxen V Star, LHXL-LB5C), each equipped with a small reflector, short pass filter (505 nm) and cooling fan. The LEDs were ~80 mm from the heart surface. The LEDs were driven at 700 mA using a power supply (POWERTECH, MP3087) in current control mode and were allowed to stabilize for at least 60 minutes before measurements were made.

The heart was imaged using a cooled EMCCD camera (Cascade 128+, Photometrics) at 128x128 pixels, 16bit resolution and 326 frame/s. The camera was equipped with a zoom lens (Navitar NAV DO-5095), x2 close up lens (B+W, NL-2) and long pass filter (600nm, Marumi MC-R2). The camera was positioned ~220mm from the heart providinga field of view of 20 by 20 mm at a spatial resolution of 156 μm^2 per pixel. Camera acquisition was controlled with a laboratory PC using V++ software (Digital Optics).

C. Data processing

All data were recorded at full resolution in "TIFF" format. Time series data for each pixel were processed as follows. Signals were averaged across 6 successive "periods" each synchronized with the action potential (AP) [4]

$$y(i) = \frac{1}{M} \sum_{j\ 0}^{j=M-1} \left[x_j(i) \right], i = 0,1,2,.., N \quad (1)$$

where the window M = 6 and N is the period length.

Signals were separated into a series of "periods" each containing an AP and synchronized across all pixels from the AP upstroke detected at one location.

Signal characteristics associated with heart wall motion were investigated in specific regions using individual pixel and area weighted average signals. Area weighted average signals were computed by first removing the DC offset from each pixel signal, normalizing each and computing the mean of these transformed pixel signals $x_{jT}(i)$ across a particular region

$$z(i) = \sum_{j-0}^{A} \frac{1}{A} \left[x_{jT}(i) \right] \quad (2)$$

where A is the number of pixels in the region

D. Image registration

Motion artifacts are caused in part by physical translation of heart regions with respect to the photodetector. Planar transformation of successive images to preserve the registration of key structural features provides a means of correcting for this [5]. That is, if we have separate images of the heart surface **B** and **A** that differ as a result of contraction, it may be possible to correct for the effects of heart wall motion using established image registration methods that transform **A** to best match **B**.

This process is described by the equation

$$\alpha_0 = \arg\max_{\alpha} .c\left(B(x_B), A'(T_\alpha(x_A))\right) \quad (3)$$

where the geometric transform $\mathbf{T}_\alpha$, controlled by the parameter vector α, is used to map image **A** onto **A'**. Criterion **c** defines a measure of image similarity and the vector α_0 maximizes that criterion [8].

Rohde et al. [1] used mutual information [6] as their measure of image similarity, but we use the cross-correlation coefficient. This criterion is reliable and robust in the presence of variable image intensity [7].

The cross-correlation coefficient is estimated [8] as

$$\frac{\sum_i (a_i - \bar{a})(b_i - \bar{b})}{\sqrt{\sum_i (a_i - \bar{a})^2 \sum_i (b_i - \bar{b})^2}} \quad (4)$$

where

$$\bar{a} = \frac{1}{N} \sum_i a_i \quad \text{and} \quad \bar{b} = \frac{1}{N} \sum_i b_i$$

and N is the number of pixels.

Bilinear interpolation was applied to images. In this initial proof-of-concept study, a simple 3 parameter transformation that allowed rotation as well as translation in both axes was used for image registration in small regions of interest (ROI) only.

For analysis purposes a graphics user interface (GUI) application was designed in the computing environment MATLAB (ver. R2007B). This enabled analyses to be carried out and results displayed in user defined regions of interest (ROI).

III. Results

In this study, fluorescence signals were acquired from isolated beating hearts in the absence of pharmacological uncouplers or mechanical restraint. Image intensities are represented in pseudocolour with red indicating maximum and blue minimum intensities.

Figure 1 shows the first frame of raw and time-averaged (M=6) signals. The epicardial surface of the left ventricle (LV) can be seen on the right-hand side of the frame and variation in staining intensity (red to light blue) is evident.

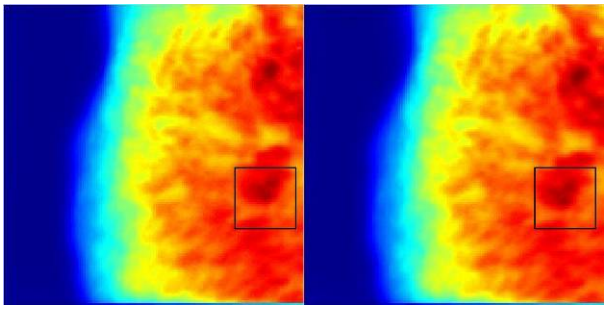

Figure 1. Single frame (20 x 20 mm, 128 x128 pixels) containing LV epicardial surface: **A** raw and **B** time-averaged (M=6) images. The black square shows ROI 25 by 25 pixels.

In Figure 2, below, time-averaged signals (M=6) are presented for the 25 x 25 pixel ROI in Figure 1. DC offset is removed and signals are normalized. Area weighted signals (2 x 2 pixels) are presented for four locations within the region. All four exhibit a sharp initial negative deflection followed by a slower wave of variable polarity. The first deflection reflects the "red" shift in the fluorescence emitted by the membrane-bound dye di-4 ANEPPS as a result of

depolarization. and the arrow indicates the direction of the wall motion. The subsequent slower wave is due to the contraction of the heart. It is due in part to the movement of regions of the heart surface with varying stain intensity with respect to the photodetector array.

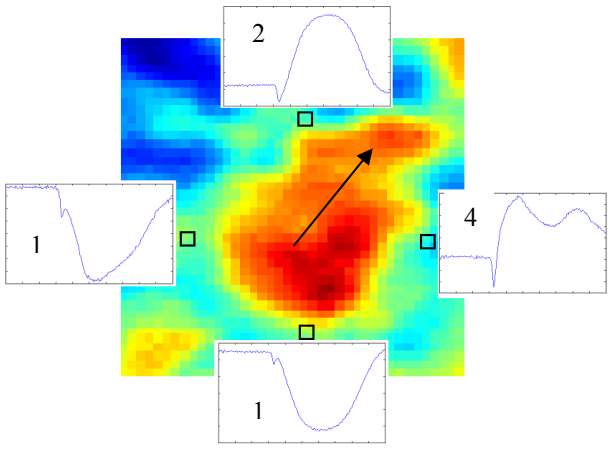

Figure 2. Time-averaged (M=6) fluorescence signals in the ROI. Time series signals from the four 2 x 2 pixel squares indicated show membrane potential modulation and motion artifacts. The arrow shows the direction of the wall motion. The graphs horizontal axes shows time, vertical axes shows signal intensity.

In order to understand the factors which contribute to this artifact more fully, the image registration technique outlined in the Methods section was used to suppress frame-to-frame motion of the heart within the ROI. In the upper panel of Figure 3, the movement of a readily identified structural feature is tracked through a cycle of contraction in frames separated by 46 ms. There is evident transformation of the image throughout this period. In the lower panel of Figure 3, corresponding frames are shown after image registration. Key features within the image have been stabilized.

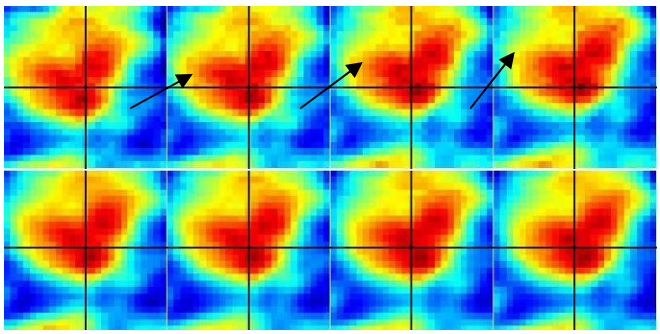

Figure.3. Suppression of cardiac motion in ROI using image registration. Upper panel: Frames at 46 ms intervals through cardiac cycle without image registration. Arrow tracks the registered path on the heart surface. Lower panel: Corresponding frames after image registration. The cross hairs provide a fixed spatial reference.

In Figure 4, time-averaged signals are presented after image registration for the four locations shown in Figure 2. As the result of image registration, motion artifact has been substantially reduced. The Figure 4 shows the signals from image registered sequence at the same position as are depicted in figure 2. The characteristic spike of the rat cardiac action potential is now evident, although additional high frequency noise has been introduced into the signals.

Figure 5 shows area weighted average signals across the full 25 x 25 pixel ROI, before (blue) and after (red) image registration. It is noteworthy that motion artifact appears to be suppressed in both

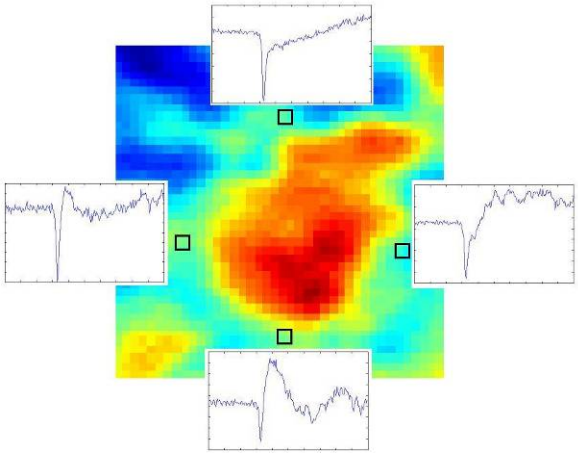

Figure 4. Time-averaged fluorescence signals in the ROI after image registration. Time series signals from the same four locations in Figure 2 exhibit much less motion artifact. The graphs horizontal axes shows time, vertical axes shows signal intensity.

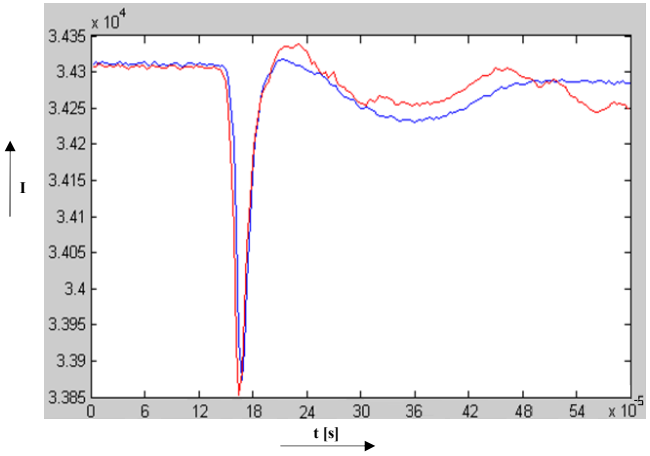

Figure 5. Area weighted average signals across the ROI before (blue) and after (red) image registration. The graph horizontal axes shows time, vertical axes shows absolute signal intensity (the scale is 16 bit unsigned integer).

IV. DISCUSSION

In this study we have characterized the signals acquired by optical mapping from the surface of the beating rat heart in the absence of electromechanical uncouplers or physical restraint. As expected, electrical modulation of the fluorescence signal is swamped by artifact that results from the mechanical contraction of the heart. Our results suggest that this artifact is principally due to two factors (i) nonuniform staining resulting in variable intensity of background fluorescence emission from different regions of

the heart and (ii) motion of the heart surface with respect to the photo-detector. Motion artifact is relatively slow in comparison to modulation caused by electrical activation and is most marked adjacent to regions where intensity gradients are greatest. As shown in Figures 2 and 3, the polarity of the artifact depends on the motion of the image. Thus as intensely stained tissue traverses the 2 x 2 pixel subregion toward the top of Figure 2 the average signal across these pixels increases, whereas the average signal falls in the equivalent subregion toward the bottom of Figure 2 as more intensely stained tissue moves out. Consistent with this, motion artifact is not evident across regions of the heart surface that are uniformly stained.

This view is supported by the image registration results. Using a simple linear transformation (see Figure 4), it was possible to preserve spatial registration within a subregion of the image field and motion artifact was substantially reduced as a result. Residual motion artifact after correction is likely due to the fact that the heart wall motion captured by a planar imaging system cannot be described fully by a linear transformation. However, by tracking the motion of multiple subregions of appropriate dimension within the image, it is entirely possible to identify nonlinear transformations that provide more precise image registration. We hypothesize that the use of such an approach could lead to substantial additional suppression of motion artifact.

A strength of such an approach is that background information only is used to track regional heart wall motion and image registration is achieved by mapping nonuniformly stained regions so that they match each other on a frame-to-frame basis. Other characteristics of motion artifact may also be used to facilitate the process of its removal. We have shown that motion artifact can be reduced by summing fluorescence signals across a closed region. It also follows that the spatial gradient of the motion component of fluorescence signals carries detailed information on regional heart wall motion. We argue that the combined use of this image information should provide an efficient means of maintaining image registration in the beating heart and therefore enable reliable measurement of electrical activity using optical mapping in the absence of electro-mechanical uncouplers and physical restraint.

V. Conclusion

In this study, features of the artifact observed during optical mapping of the beating heart have been characterized. Image registration techniques have been shown to suppress these artifacts and more comprehensive methods for removal of motion artifact are discussed .

References

[1] EFIMOV, R. I., NIKOLSKI, P. V., SALAMA,G. Optical Imaging of the Heart, In Circulation Research 2004. Vol. 95, p. 21-33.

[2] KINSLEY, Stephen B., et al. Ratiometry of transmembrane voltage-sensitive fluorescent dye emission in hearts, In American Journal of Physiology Heart and Circulatory Physiology, 2000. Vol. 279, p.1421-1433.

[3] TAI, Dean C.-S., et al. Correction of motion artifact in transmembrane voltage sensitive fluorescent dye emission in hearts. In American Journal of Physiology Heart and Circulatory Physiology, 2004. Vol. 287, p. 985-993.

[4] JAN, J. Digital Signal Filtering, Analysis and Restoration. Institution of Electrical Engineers, 2000. ISBN 0852967608

[5] RHODE, G. K., DWANT, B.M. LIN, S. Correction of motion artifact in cardiac optical mapping using image registration, In IEEE Transaction on Biomedical Engineering , 2005. Vol. 52, Is.2, p. 338-341.

[6] MAES, Frederik, et al. Multimodality Image Registration by Maximization of Mutual Information. In IEEE Transactions of Medical Imaging, 1997. Vol. 16, No.2., p. 187-198.

[7] JÄHNE, B. , Digital Image Processing, 6th revised and extended edition, Springer-Verlag Berlin Heidelberg , 2005, ISBN 3-540-24035-7

[8] JAN, J. Medical Image Processing Reconstruction and Restoration, Concepts and Methods, CRC Press, 2006, ISBN 0-8247-5849-8